Dalton Trans., 2018, 47, 13229–13238 - DOI: 10.1039/c8dt03169j

Journal Name

ARTICLE

# Salen, Salan and Salalen Iron (III) Complexes as Catalysts for $CO_2$/Epoxides Reactions and ROP of Cyclic Esters

Received 00th January 20xx,
Accepted 00th January 20xx

DOI: 10.1039/x0xx00000x

Mariachiara Cozzolino,[a] Vincenza Leo,[a] Consiglia Tedesco,[a] Mina Mazzeo[a] and Marina Lamberti*[b]

Salen ligand and its derivatives salan and salalen, bearing the same substituents on the phenolate rings, have been synthesized and then used for the preparation of the corresponding Fe(III) complexes. All complexes were characterized by MALDI ToF mass spectroscopy, Evans method, UV-vis and IR spectroscopies. Moreover, for the salalen-based iron complex the X-ray structure was collected. A comparison of their behaviour in the catalysis of $CO_2$ with benchmark epoxide substrates allowed us to individuate an order of reactivity of the different classes of complexes. A salen Fe(III) complex was prepared with a longer bridge between the two nitrogen atoms of the ligand skeleton in order to evaluate the influence of the flexibility on the activity of the catalyst. Finally the same complexes were tested as catalysts in the ring-opening polymerization of L-lactide and ε-caprolactone.

## Introduction

Environmental issues mainly due to human activities, such as pollution, deforestation, and global warming, pushed researchers towards the implementation of sustainable processes, that is, for example, processes using renewable and non toxic feedstocks and producing as little waste as possible.[1] Carbon dioxide is abundant, inexpensive, non toxic and renewable. Thus, the capture and the use of massive quantities of $CO_2$ as a C1 building block is a challenging goal for the fixation of this gas into useful products. The reaction of $CO_2$ with epoxides is a 100% atom efficient process furnishing cyclic carbonates and/or polycarbonates. Cyclic carbonates (CCs) have a significant commercial interest owing to their several uses, such as, electrolytes in lithium-ion batteries, polar aprotic green solvents, and intermediates for the synthesis of polymers and fine chemicals.[2-7]

Ring-opening polymerization of lactones and lactides is a process which allows the production of biodegradable polymers from renewable resources. Polylactones and polylactides find application both as commodities, for example, in green packaging, and, thanks to their biocompatibility, in the niche market of biomedical and pharmaceutical industries.[8-13]

One of the goals in realizing a sustainable process is the reduction of energy demand. From this point of view the catalyst plays a fundamental role, since it allows to carry out the reactions in reduced time and under milder reaction conditions. Usually, metallic complexes employed as homogenous catalysts have the general formula $L_nMX_m$, in which $L_n$ is a set of ancillary ligands which tune the electronic and steric properties of the metal complexes, R is an initiating group, and M is the active metal center. Thanks to the nearly unlimited supply and its biocompatibility, iron is one of the metals of choice in several catalyzed reactions.[14] However, to date, only limited examples of iron complexes have been reported as catalysts either in the $CO_2$/epoxide reactions or in the ROP of cyclic esters. Scientific literature dealing with $CO_2$/epoxide reaction promoted by iron-based systems mainly described complexes with phenoxy-based ancillary ligands at variable denticity (i.e. Robson-type,[15] amino triphenolate,[16-18] pyridylamino-bis-phenolate,[19] thioether-triphenolate,[20-21] bis-phenoxyimine[22,23] and phenoxyamine ligands[24]). In other cases, neutral or anionic nitrogens were the donor atoms of the chelating ligand (i.e. iminopyridine[25], bis-CNN pincer,[26] tetraamine,[27] bis-aminepyridine[28] and bis-imido[29] ligands). One paper also described the use of simple iron salts to convert epoxidized vegetable oils into biobased cyclic carbonates.[30] These works showed the propensity of iron complexes to promote the coupling of epoxides and $CO_2$ towards the formation of cyclic carbonates. As exceptions, some complexes were also found to be able to switch their selectivity towards polycarbonates, when operating with internal epoxides, by changing the reaction conditions.[15,18,19]

[a] Dipartimento di Chimica e Biologia "A. Zambelli", Università di Salerno, via Giovanni Paolo II 132, I-84084, Fisciano, Salerno, Italy
[b] Dipartimento di Fisica "E. Caianiello", Università di Salerno, via Giovanni Paolo II 132, I-84084, Fisciano, Salerno, Italy.

Electronic Supplementary Information (ESI) available: Synthetic procedures and spectra of the complexes, additional catalysis data and NMR spectra of the polyesters are reported. CCDC-1858978 contains the supplementary crystallographic data for this paper See DOI: 10.1039/x0xx00000x

Dalton Trans., 2018, 47, 13229–13238 - DOI: 10.1039/c8dt03169j



On the other hand, iron-based systems promoting ROP of lactones and/or lactides consist predominantly of inorganic or organic iron salts, such as, for example, oxides,[31] halides,[32-33] carboxylates,[34] alkoxides,[35-37] and lactate.[38] However, some examples of $L_nMX_m$ complexes, bearing ancillary ligands, have been reported also in this catalysis (for example, $L_n$ = benzamidinate,[39] iminopyridine,[40] β-ketimine,[41] NNN-pincer,[42] β-diminate,[43] calixarene[44] and N-heterocyclic carbene[45] ligands).

Salen based complexes are ubiquitous in several kinds of catalysis, since they are cheap, facile to synthesize, and may be easily modulated whether from a steric or electronic point of view. Salan and salalen ligands are salen derivatives which show similar advantages of their oxidized counterpart, nevertheless they have been much less explored. The different hybridization of the nitrogen atoms in these classes of tetradentate ligands may differentiate the behaviour of the corresponding complexes in a substantial way.

Salen-based iron complexes with aromatic bridge, have been described as catalysts in the production of styrene carbonate from $CO_2$ and styrene oxide.[46] Other authors reported the reactivity of salen iron complexes in the ROP of lactides and caprolactone showing the dependence of the activity on the substituents of the phenoxy moieties and, for caprolactone, also on the bridge between the nitrogen atoms.[47]

Salan-based iron complexes with homopiperazine bridge and different substituents on the aromatic rings have been reported by Kerton, and showed good activities in the production of cyclic carbonates from $CO_2$ and epoxides.[48]

Our interest in the study of salen- and its derivatives- based aluminum complexes both in the ROP of cyclic esters[49-51] and in the $CO_2$/epoxide reactions[52,53] induced us to explore the behaviour of iron complexes in these same reactions.

In this paper we synthesized salen, salan and salalen iron (III) complexes, choosing ligands with alkyl bridges and the same substitution pattern on the phenoxy moieties. The paramagnetic iron complexes have been characterized by UV-vis and IR-spectroscopies, MALDI-ToF mass spectrometry and measurement of magnetic moments by Evans' method. All complexes have been first tested in the reaction of $CO_2$ with benchmark epoxides (such as, cyclohexene oxide, propylene oxide, and styrene oxide) and subsequently in the ring-opening polymerization of L-lactide and ε-caprolactone, with the aim to compare their behaviour in catalysis.

## Results

### Synthesis and Characterization of Complexes 1-4

Complexes **1**-**4** (Fig. 1) were synthesized by direct reaction of ligand precursors and $FeCl_3$ in the presence of triethylamine, carrying out the reaction in dry methanol.

Complexes **1**,[54,55] **2**[47,56,57] and **4**[47] were previously reported in the literature while complex **3** is a new species. The paramagnetic complexes were firstly analyzed by MALDI-ToF mass spectroscopy. For the salen-iron complex **2** the most intense peak was that attributable to the molecular ion while for the salan, salalen- and the salenC3- iron complexes **1**, **3** and **4** the higher peak corresponded to the species formed after the loss of one chloride (Fig. S1-S8 in the ESI).

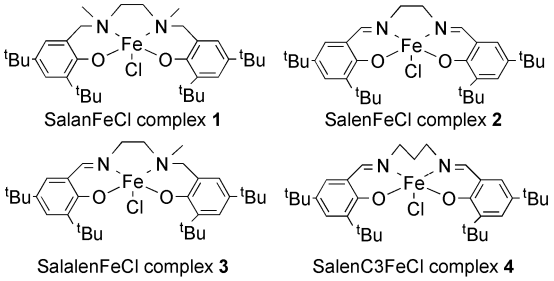


Fig. **1** Complexes **1**-**4** studied in this paper.

Both ligand precursors and complexes **1**-**4** were analyzed by UV-visible spectroscopy. All samples were dissolved in acetonitrile (80 μmol) and absorbance was recorded from 200 to 1000 nm (see Fig. S9-S10 in the ESI and Fig. 2).

Spectra of complexes **1** and **2**, and of the related ligands, were in agreement with those reported in the literature.[55,57] In particular, the spectrum of salanFeCl (complex **1**) exhibits an absorption band at 281 nm, which was found also in the spectrum of the free salen ligand and was therefore assigned to a $\pi \rightarrow \pi^*$ transition of the phenolic chromophores, and two absorption bands at lower energy (337 and 552 nm) and with low intensities corresponding to phenolate ligand-to-metal charge-transfer (LMCT) transitions. For complex **2** (salenFeCl), two bands at 265 and 327 nm were assigned to $\pi \rightarrow \pi^*$ transitions of the phenolic chromophores. While an absorption band at lower energies (504 nm), absent in the spectrum of the free ligand, was assigned to a phenolate LMCT transition.

The spectrum of the salalen ligand presented both the bands of the salen and of the salan ligands although with a half intensity (Fig. S9 in the ESI). This observation is perfectly coherent with the fact that the salalen is a hybrid structure between salan and salen, containing both the amine and the imine moieties. The salalenFeCl complex **3** showed two absorption bands at 270 and 329 nm deriving from transitions of the phenolic chromophores, and a band at 524 nm due to a

**Fig. 2** Electronic absorption spectra of complexes **1**-**3** in acetonitrile (80 μmol).

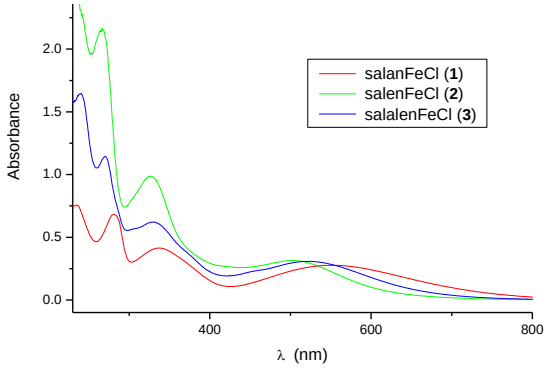

Dalton Trans., 2018, 47, 13229–13238 - DOI: 10.1039/c8dt03169j



phenolate LMCT transition.

Finally, salenC3FeCl complex **4** showed three bands at 242, 273 and 332 nm, due to the ligand transitions, and one LMCT transition at 520 nm (Fig. S10 in the ESI).

The energy of absorption of the LMCT bands gives an indication of the Lewis acidity of the iron center. In particular, a lower energy should indicate a higher acidity of the metal.[45] Comparing the observed transitions for complexes **1**-**3**, the data indicate the following order of acidity: salanFeCl **1** > salalenFeCl **3** > salenFeCl **2**.

The IR spectra of ligands and complexes **1**-**4** were acquired by mixing the solid samples with KBr, and are reported in Figures S11-S13 in the ESI. Salen, salalen and salenC3 ligands show peaks attributable to C=N stretching at 1629, 1632 and 1634 $cm^{-1}$ respectively. For the corresponding complexes, **2**, **3** and **4**, these peaks shift at 1610, 1614 and 1609 $cm^{-1}$, respectively, indicating the accomplishment of the ligand coordination to the iron metal. Moreover, the spectrum of each complex, compared to the spectrum of the corresponding ligand, shows the appearance of two peaks around 540 and 480 $cm^{-1}$ indicative of the presence of M-N and M-O bonds, respectively, thus corroborating the coordination of the ligand to the metal. Finally, as predictable, the IR spectra of salalen ligand and complex **3**, can be seen as the sum of the salan and salen corresponding spectra.

The magnetic susceptibility data for complexes **1**-**4** were determined at room temperature by Evan's NMR method by using $C_6D_6$ as solvent and cyclohexane as diamagnetic reference. The magnetic moments of complexes **1**-**4** were in the range 5.3-6.0 and thus close to the spin-only value of 5.92 $\mu_B$ for S=5/2, indicating the formation of high-spin Fe(III) complexes.

**Single-crystal structure analysis**

Purple prismatic single crystals of the complex **3** suitable for X-ray diffraction analysis were obtained by slow evaporation of acetone.

The X-ray molecular structure is shown in Fig. 3. Selected bond lengths and angles for complex **3** and analogous complexes **1**[55] and **2**[47] are reported in Table S1 in the ESI.

The Fe atom in complex **3** is five-coordinate, adopting a distorted trigonal bipyramidal (tbp) geometry. The O1 and N2 atoms occupy the apical positions, while the N1, O2 and Cl atoms lie in the equatorial plane (Fig. 3).

The tbp geometry was assessed using the geometric parameter $\tau = |\beta - \alpha|/60$, where β = N1—Fe—O2 angle and α = N2—Fe—O1 angle (see Scheme 1). A value of zero applies to a compound with a perfect square-pyramidal (sqp) geometry and a value of 1 to a perfect tbp geometry. For complex **3** τ is 0.78, interestingly for complex **1** τ is 0.31 indicating a distorted sqp geometry, while for complex **2** τ is 0.47.

The methyl C atom lies on the same part as the Cl atom deviating from the N1FeN2 mean plane by 0.95 Å. The bridge C atoms (C16 and C17) are on the opposite sides with respect to the N1FeN2 mean plane and deviates from it by 0.31 Å and 0.33 Å, respectively.

As for complex **1**, the methyl groups are on the opposite side with respect to the N1FeN2 mean plane deviating by 1.22 and

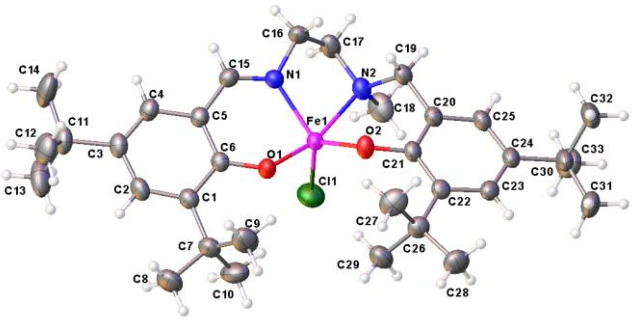


**Fig. 3** ORTEP diagram of complex **3**. Ellipsoids are drawn at 50% probability level.

1.36 Å. As for the bridge C atoms, one deviates from the mentioned plane by 0.60 Å and the other only by 0.09 Å.

Similarly to **1** also in complex **2** one bridge C atoms deviates by 0.68 Å and the other only by 0.09 Å.

As for the Fe-N1 and Fe-N2 distances in the three complexes, the following trends **1**>**2**>**3** and **3**≈**1**>**2** (confirmed by standard deviations) can be determined, respectively. Whereas, less significant differences resulted for the Fe-O1, the Fe-O2 and the Fe-Cl distances. Since longer distances indicate weaker bonds and thus more acidic iron center, the following order of acidity salanFeCl **1** > salalenFeCl **3** > salenFeCl **2** can be inferred for the examined complexes, in agreement with what gathered from the LMCT band of the electronic absorption spectra.

**Catalytic cycloaddition of carbon dioxide with epoxides**

Subsequently, the performance of complexes **1**-**4** were tested in the reaction of $CO_2$ with benchmark epoxides, namely propylene oxide, styrene oxide and cyclohexene oxide as representative, respectively, of terminal, aromatic and internal epoxides (Scheme 1). Reaction conditions and obtained conversions of the reaction of $CO_2$ with propylene oxide are reported in Table 1.

All complexes were active and selective in the cycloaddition reaction by furnishing propylene carbonate (PC) as exclusive product. The first experiment was carried out with complex **1** in the presence of tetrabutylammonium bromide (TBAB) as cocatalyst (see Entry 1 in Table 1), under the same reaction conditions used for the salanFeCl complex reported by Kerton. Our complex was found to be more active (TOF = 213 $h^{-1}$) than that reported in the literature (135 $h^{-1}$).[48] We tested the same complex with a lower amount of TBAB (cf entries 1-3 in Table 1). As expected, by lowering the equivalents of cocatalyst the conversion decreases. We evaluated the use of 2 equivalents

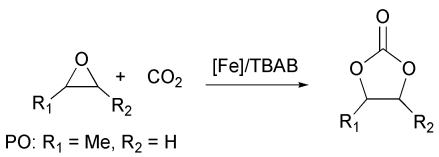


PO: $R_1$ = Me, $R_2$ = H

SO: $R_1$ = Ph, $R_2$ = H

CHO: $R_1$ $R_2$ = -$(CH_2)_4$-

**Scheme 1** Coupling reaction of epoxides with $CO_2$

as a good compromise to get high conversion while saving up the cocatalyst.

Afterwards, we tested complexes **2** and **3**, bearing, respectively, salen and salalen ligands, under the same reaction conditions (see entries 4-5 in Table 1), obtaining the following order of reactivity: salanFeCl **1** >salenFeCl **2** > salalenFeCl **3**. This was quite unforeseen since the salalen ligand has a hybrid structure between salan and salen, consequently an intermediate reactivity for the corresponding iron complexes would have been expected. The same order of reactivity, was observed by comparing the behaviour of complexes **1**-**3** as catalysts in the $CO_2$/PO reaction carried out by using bis(triphenylphosphoranylidene)ammonium chloride (PPNCl) as cocatalyst (see Table S2 in the ESI).

Reasoning on the higher activity of complex **1**, bearing an ethylene bridge between the two nitrogen atoms, with respect to the salanFeCl reported in the literature with a more rigid homopiperazine based bridge,[48] we hypothesized a role of the flexibility on the reactivity of the cited complexes. To verify this speculation, we performed the synthesis of complex **4**, an iron chloride complex bearing a salen ligand with a propylene bridge between the two nitrogen atoms and thus with a higher flexibility with respect to complex **2**. The reaction of PO with $CO_2$ carried out in the presence of complex **4** under the same reaction conditions of complex **2** (cf entries 4 and 6), showed a higher activity of this catalyst, and comparable to that of complex **1**, corroborating the importance of the flexibility of the ligand skeleton on the catalyst performance. Finally, we demonstrated the requirement to use both the catalyst and the cocatalyst to get the active species, by conducting two reference reactions in the presence of TBAB alone or of complex **4** alone. Under these conditions low conversions were observed (compare entries 7 and 8 with entry 6 in Table 1).

Table 1. $CO_2$/PO reaction promoted by complexes **1**-**4** and tetrabutylammonium bromide (TBAB). [a]

| Entry | Cat | TBAB (eq) | Conversion (%) | TON | TOF ($h^{-1}$) |
|---|---|---|---|---|---|
| 1 | **1** | 4 | 85 | 3400 | 213 |
| 2 | **1** | 1 | 58 | 2320 | 145 |
| 3 | **1** | 2 | 77 | 3080 | 192 |
| 4 | **2** | 2 | 64 | 2560 | 160 |
| 5 | **3** | 2 | 44 | 1760 | 110 |
| 6 | **4** | 2 | 78 | 3120 | 193 |
| 7 | - | 2 | 24 | - | - |
| 8 | **4** | - | 12 | | |

[a] **General conditions:** Complexes: **1**-**4** = 17.5 µmol (0.025mol%), PO = 5 mL (4000 equiv), $Pco_2$ = 20 bar, Temperature = 100°C, time = 16 h.

Subsequently, complexes **1**-**4** were used as catalysts in the reaction of $CO_2$ with styrene oxide (SO) and cyclohexene oxide (CHO). For these reactions, due to the lower reactivity of SO and CHO with respect to PO, 4 equivalents of TBAB were used. Moreover, for the CHO, which is an internal epoxide and, hence, usually showing a very low reactivity, a longer reaction time was set. The results are reported in Table 2. In all cases, cyclic carbonates were obtained as exclusive products (*cis*-CHC in the case of CHO).

Table 2. Reaction of $CO_2$ with styrene oxide (SO) and cyclohexenoxide (CHO) promoted by complexes **1**-**4** and tetrabutylammonium bromide (TBAB). [a]

| Entry | Cat | Epoxide | Conversion (%) | TON | TOF ($h^{-1}$) |
|---|---|---|---|---|---|
| 1 | **1** | SO | 53 | 2120 | 132 |
| 2 | **2** | SO | 46 | 1840 | 115 |
| 3 | **3** | SO | 44 | 1760 | 110 |
| 4 | **4** | SO | 53 | 2120 | 132 |
| 5 | - | SO | 15 | - | - |
| 6 | **1** | CHO | 19 | 760 | 35 |
| 7 | **2** | CHO | 18 | 720 | 32 |
| 8 | **3** | CHO | 13 | 520 | 24 |
| 9 | **4** | CHO | 19 | 760 | 35 |
| 10 | - | CHO | 10 | - | - |

[a] **General conditions:** Complexes: **1**-**4** = 17.5 µmol (0.025mol%), Epoxide = 4000 equiv (7 mL of CHO, 8 mL of SO), $Pco_2$ = 20 bar, Temperature = 100°C, time = 16 h for SO, 22 h for CHO.

In particular, the *cis*-CHC products were obtained with low conversions resulting in a depression of the differences among the different complexes. Anyway, also with these less reactive epoxides the order of activity was the same observed in the case of the PO/$CO_2$ reaction, i.e. salenC3FeCl **4** ≥ salanFeCl **1** > salenFeCl **2** > salalenFeCl **3**.

**Ring Opening Polymerization of ε-caprolactone and L-lactide**

Next the behaviour of complexes **1**-**4** as catalysts in the Ring Opening Polymerization (ROP) of L-lactide and ε-caprolactone, was explored (Schemes 2 and 3).

As described in the literature,[47,58] metal chloride are not good initiators in the ROP of lactide, however PO can promote the *in situ* formation of an active alkoxide species also being a good solvent for this reaction. On the basis of this hint, a catalytic

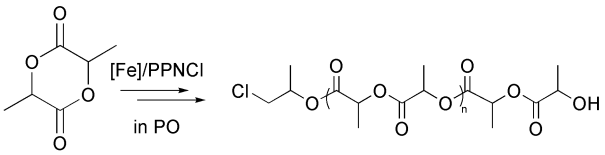


**Scheme 2** Ring opening polymerization of L-LA.

Dalton Trans., 2018, 47, 13229–13238 - DOI: 10.1039/c8dt03169j



experiment was carried out in PO. After 4 hours, 33% of 100 equivalents of L-LA were converted in PLLA, operating at 60 °C (entry 1 in Table S3 in the ESI). According to different authors,[58-60] the coordination of the PO to the metal would activate the epoxide to the nucleophilic attach by the chloride (bonded to the metal or deriving from an exogenous source), this would result in the opening of the epoxide and in the formation of a metal alkoxide species which, in turn, will promote the ring opening polymerization of the cyclic ester. This picture was confirmed through the end group study of the obtained polymers by $^{1}H$ and $^{13}C$ NMR analysis (Fig. S14-S15 in the ESI). In particular, signals were observed which correspond to the initiating groups generated by ring-opening of PO by chloride (−$OCHCH_3CH_2Cl$)[47] and peaks which correspond to hydroxyl end groups (-$OC{=}OCHCH_3OH$), generated by hydrolysis of the polylactyl growing chain (Scheme 2).‡ With the aim to increase the rate of the initiating step, i.e. the opening of the PO, PPNCl was added to the reaction medium, as an exogenous source of the nucleophile. Thus, by carrying out the polymerization of L-LA under the same conditions detailed for the previous polymerization, but in the presence of one equivalent of PPNCl, a conversion of 63% was reached in 4 hours (entry 2 in Table S3 in the ESI) indicating a doubling of the activity. Also in this case, the $^{1}H$ and $^{13}C$ NMR spectra showed the presence of end groups confirming the proposed mechanism. Afterwards, carrying out polymerization experiments, under the same experimental conditions, in the presence of either complex **1** or complex **3,** no conversion was observed in both cases (entries 3 and 4 in Table S3 in the ESI). A complete lack of activity from such structurally similar complexes was quite surprising.

Thus, we decided to explore the behaviour of the synthesized complexes in the ROP of ε-caprolactone, which is still a cyclic ester but with significant differences with respect to lactide (e.g., less steric encumbrance, lack of the possibility to form bis-chelated intermediates, usually higher reactivity).

Polymerization experiments of ε-caprolactone conducted in the presence of complexes **1**-**3** in PO as solvent and at room temperature, gave the results summarized in Table 3. After 8 hours, $^{1}H$ NMR spectra of small aliquots of the polymerization mixtures, showed a conversion of 78% for the salanFeCl complex **1**, while complexes **2** and **3** showed no activity. Prolonging the reaction time to 30 hours and 24 hours respectively for complex **2** and **3**, we managed to get an appreciable amount of polymer in both cases. The conversions showed, in these polymerization reactions, an order of reactivity as follows: salanFeCl **1** > salalenFeCl **3** > salenFeCl **2**. Afterwards, we carried out polymerization experiments under the same reaction conditions of entries 1-3 but in the presence of PPNCl as the exogenous source of the chloride. In this case, after 8 hours, complexes **2** and **3** showed higher conversions with respect to the same experiments conducted without PPNCl (cf entries 5 and 6 vs 2 and 3) while a negligible difference was observed for complex **1** (cf entry 4 vs 1). For longer reaction time, complex **2** showed an activity comparable to that in the absence of PPNCl (cf entry 5 vs 2), while complex **3** showed and improved activity (cf entry 6 vs 3). Thus, also in the presence of PPNCl as cocatalyst, the order of reactivity resulted: salanFeCl **1** > salalenFeCl **3** > salenFeCl **2.** Finally, a polymerization experiment carried out with PPNCl alone showed that, under the same reaction conditions, this species did not show any activity (entry 7).

The obtained polycaprolactones were examined by NMR spectroscopy and GPC analysis. $^{1}H$ and $^{13}C$ NMR analysis (Fig. S16 and S17 in the ESI) revealed the presence of initiating groups generated by ring-opening of PO by chloride (−$OCHCH_3CH_2Cl$) and followed by insertion of the monomer unit into the so formed iron-oxygen bond with cleavage of the acyl−oxygen bond of the monomer and hydroxyl end groups ($CH_2CH_2OH$; 3.62 ppm), generated by hydrolysis of the growing chain (Scheme 3). The integration of this signal of the end group (3.62 ppm) with respect to the signal at 2.30 ppm of the repetitive unit, allowed us to calculate the molecular weight of the PCL sample ($M_n^{NMR}$ in Table 3). Theoretical molecular weights ($M_n^{th}$ in Table 3) were calculated assuming that a single PCL chain is produced per metal center through initiation of the polymerization by the opened propylene oxide group (−$OCHCH_3CH_2Cl$). Moreover, the samples were analyzed by GPC to determine the $M_n^{GPC}$ and the dispersities (Đ). All the obtained PCLs possess quite narrow molecular weight distributions (Đ = 1.07−1.56) with unimodal characteristics. The good agreement between the $M_n$ values determined both by GPC and by NMR with the theoretical molecular weights, indicated the occurrence of a controlled polymerization which proceeds exclusively by the mechanism detailed above. As exception, PCL sample obtained by salalenFeCl complex **3** in the absence of PPNCl (entry 3) showed experimental molecular weights ($M_n^{NMR}$ and $M_n^{GPC}$) almost twice those calculated by the converted monomer units ($M_n^{th}$) suggesting a low initiation efficiency.

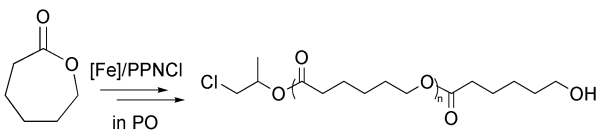


**Scheme 3** Ring opening polymerization of ε–caprolactone.

Dalton Trans., 2018, 47, 13229–13238 - DOI: 10.1039/c8dt03169j



Table 3. ROP of ε-caprolactone promoted by complexes **1**-**4** and PPNCl.

| Entry | Cat/ Cocat | Time (h) | Conv (%) | $M_n^{th}$ (KDa)[a] | $M_n^{NMR}$ (KDa) | $M_n^{GPC}$ (KDa)[b] | Đ [b] |
|---|---|---|---|---|---|---|---|
| 1 | **1**/ - | 8 | 78 | 8.8 | 10.2 | 12.1 | 1.07 |
| 2 | **2**/ - | 8 | 0 | - | - | - | - |
| | | 24 | 32 | - | - | - | - |
| | | 30 | 43 | 4.9 | 4.3 | 3.6 | 1.56 |
| 3 | **3**/ - | 8 | 0 | - | - | - | - |
| | | 24 | 64 | 7.3 | 13.0 | 12.3 | 1.13 |
| 4 | **1**/ PPNCl | 8 | 83 | 9.4 | 8.3 | 10.9 | 1.12 |
| 5 | **2**/ PPNCl | 8 | 6 | - | - | - | - |
| | | 30 | 45 | 5.1 | 6.7 | 4.0 | 1.50 |
| 6 | **3**/ PPNCl | 8 | 34 | - | - | - | - |
| | | 24 | 90 | 10.3 | 14.3 | 15.5 | 1.19 |
| 7 | -/ PPNCl | 8 | 0 | - | - | - | - |

**General conditions:** Complexes: **1**-**4** = 17.2 µmol, 1 equiv of PPNCl, solvent: PO = 5 mL, ε-CL= 1.7 mmol (100 equiv), room temperature. Conversion of ε-CL as determined by $^1$H NMR spectral data. [a] $M_n^{th}$ (in g mol$^{-1}$) = 114.14 × ([ε-CL]$_0$/[I]) × conversion ε-CL. [b] $M_n^{GPC}$ (KDa) and Đ values were determined by GPC in THF against polystyrene standards and corrected using the factor 0.56 $M_n^{GPC}$.

## Discussion

The mechanism of epoxide/$CO_2$ reaction in the presence of different salenM(III)Cl complexes (with M = Cr, Al and Co) has been extensively studied and reviewed.[61-63] The possible mechanism pathways, described with a model salen-complexes, contemplate, as the first step, the coordination of the epoxide in the position *trans* to the nucleophile. Afterwards, nucleophile bound to the metal of another complex (bimetallic initiation pathway) or a nucleophile purposely added to the reaction medium (binary initiation pathway) ring-opens the coordinate epoxide. After the insertion of $CO_2$ in the metal-oxygen bond, the reaction proceeds by the $S_N2$ attack of the oxygen of the carbonate group to the carbon bearing the nucleophile, thus furnishing the cyclic carbonate (Fig. 4).

To explain the difference observed with the explored complexes **1**-**3**, we compared their solid state structures. In Table S1 (ESI) the most relevant angles and distances of the three complexes were reported. In particular, the τ parameters have been calculated for each complex. These values indicated for the salanFeCl complex **1** a structure closer to a square pyramidal geometry (τ = 0.31), while the salalenFeCl **3** is better described with a trigonal bipyramidal geometry (τ = 0.78) and, finally, the salenFeCl **2** is in between these two possible geometries (τ = 0.47). As a consequence, the coordinative pocket in the position *trans* to the chloride would allocate the epoxide more easily in the order salanFeCl **1** > salenFeCl **2** > salalenFeCl **3**. The coordination of the epoxide to the metal, activates it towards the attack of the nucleophile, which is the rate determining step in the formation of cyclic carbonates. Reasonably, a more efficient

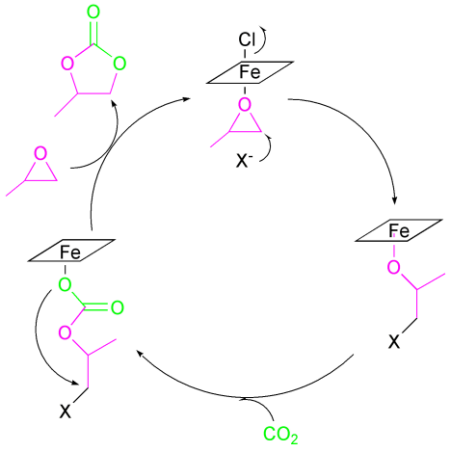


**Fig. 4** Catalytic cycle for the formation of cyclic propylene carbonate

coordination will result in a better activation of the epoxide entailing a faster formation of the product.

In the case of the ring-opening polymerization of ε-caprolactone, the initiation step would be the same described for the coupling of $CO_2$/epoxide (i.e. the coordination of the epoxide and its ring-opening by the nucleophile), on the other hand, in the polymerization reactions, the difference in the activity of the three complexes would come from the difference in the rate of the propagating steps, i.e. the repeated insertions of the monomer in the iron-alkoxide bonds (Fig. 5). As reported in the literature,[47] the activity of iron complexes in the ring-opening polymerization of ε-caprolactone, increases by increasing the acidity of the metal centre. Thus, the order of activity order observed in the ROP of ε-CL would be in agreement with the order of Lewis acidity (salanFeCl **1** > salalenFeCl **3** > salenFeCl **2**) suggested by the position of the LMCT transitions in the UV-vis spectra and by the Fe-N distances observed in the solid state structures of the three complexes. Moreover, the comparison of the polymerization experiments detailed in Table 3, after 8 hours, shows how the initiation reaction is slower for complexes **2** and **3** than for complex **1** (and how it is accelerated by PPNCl) in agreement with what observed in the PO/$CO_2$ coupling

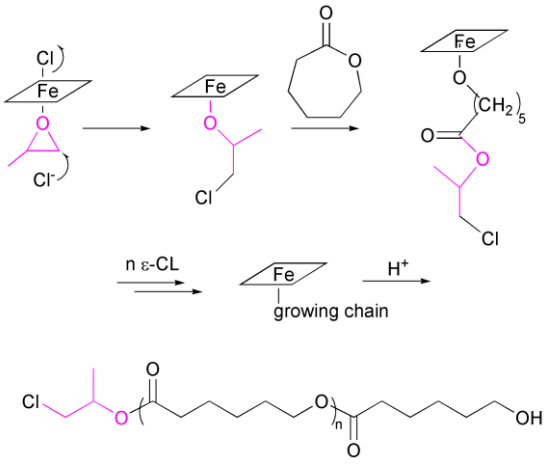


**Fig. 5** Mechanism of the ring-opening polymerization of ε-caprolactone.

Dalton Trans., 2018, 47, 13229–13238 - DOI: 10.1039/c8dt03169j



reactions.

Another aspect to clarify was the difference in the behaviour of complexes **1**-**3** observed in the ROP of L-LA and of ε-CL. Summing up, whereas in the ROP of L-LA only complex **2** showed some activity while complexes **1** and **3** were inactive, in the ROP of ε-CL complexes **1** and **3** were more active than complex **1**. As reported in the literature,[64] after the insertion of lactide into the iron alkoxide bond, an ester functionality adjacent to the growing polymer chain may form a five-membered ring chelate with the metal center (Fig. 6). Higher acidity of the metal center would determine the formation of more stable bidentate lactate intermediate. Thus, a possible explanation of the observed behaviour could be the formation of a stable lactate intermediate for the more acidic complexes **1** and **3** which hampers the insertion of other monomeric lactide units, i.e. the formation of the polymeric chain. While in the case of the less acidic salenFeCl complex **2**, the less stable lactate intermediate will allow the inserting of the lactide monomers and thus the growth of the polymeric chain.

## Experimental

### Materials and general methods

All manipulations of air- and/or moisture-sensitive compounds were carried out using standard Schlenk-line techniques under a dry nitrogen atmosphere or using a Braun Labmaster glove box. All solvents and reagents were obtained from commercial sources (Sigma-Aldrich). Anhydrous iron(III)chloride ($FeCl_3$ 99.99% purity), tetrabutylammonium bromide (TBAB, 98% purity), tetrabutylammonium chloride (TBAC, 98% purity), bis(triphenylphosphoranylidene)ammonium chloride (PPNCl) (98% purity). Methanol was distilled over sodium, propylene oxide (≥99.5%; Sigma-Aldrich), styrene oxide (97%; Sigma-Aldrich), cyclohexene oxide (98%; Sigma-Aldrich) and ε-caprolactone were distilled under reduced pressure over calcium hydride and stored in a sealed flask in a glove-box, L-lactide was purified by recrystallization from toluene.

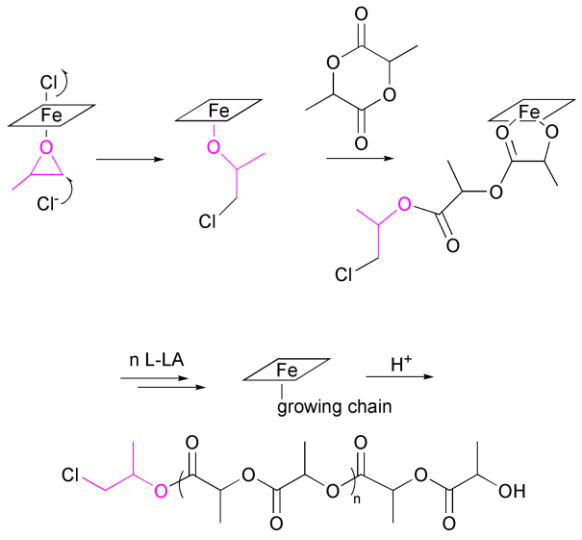


**Fig. 6** Mechanism of the ring-opening polymerization of L-lactide.

Glassware and autoclave used in the reactions were dried in an oven at 120 °C overnight and exposed to vacuum-nitrogen cycles thrice.

All other chemicals were commercially available and used as received unless otherwise stated.

### Instruments and measurements

NMR spectra were collected on Bruker Avance spectrometers (600, 400, 300, or 250 MHz for $^1$H NMR): the chemical shifts were referenced to tetramethylsilane (TMS) as external reference, using the residual protio signal of the deuterated solvents. Deuterated solvents were purchased from Sigma–Aldrich and dried over activated 3-Å molecular sieves prior to use.

The molecular weights ($M_n$ and $M_w$) and the dispersity (Đ = $M_w/M_n$) of polymer samples were measured by gel permeation chromatography (GPC) at 30 °C, using THF as the solvent, an eluent flow rate of 1 mL min$^{-1}$, and narrow polystyrene standards as the reference. The measurements were performed on a Waters 1525 binary system equipped with a Waters 2414 RI detector using four Styragel columns (range 1000–1 000 000 Å).

MALDI mass spectra were recorded using a Bruker solariX XR Fourier transform ion cyclotron resonance (FT-ICR) mass spectrometer (Bruker Daltonik GmbH, Bremen, Germany) equipped with a 7 T refrigerated actively-shielded superconducting magnet (Bruker Biospin, Wissembourg, France). The samples were ionized in positive ion modes using the MALDI ion source. The mass range was set to m/z 150–2000. The laser power was 15% and 15 laser shots were used for each scan. The samples were prepared at a concentration of 1.0 mg mL$^{-1}$ in toluene. Matrix (anthracene) was mixed at a concentration of 10.0 mg mL$^{-1}$ to promote desorption and ionization.

UV-vis spectra were recorded on a Cary-50 Spectrophotometer, using a 1 cm quartz cuvette (Hellma Benelux bv, Rijswijk, Netherlands) and a slit-width equivalent to a bandwidth of 5 nm. Measurements were performed in $CH_3CN$ at room temperature.

FTIR spectra were obtained at a resolution of 2.0 cm$^{-1}$ with a FTIR (BRUKER Vertex70) spectrometer equipped with deuterated triglycine sulfate (DTGS) detector and a KBr beam splitter, using KBr pellets disks. The frequency scale was internally calibrated to 0.01 cm$^{-1}$ using a He–Ne laser. 32 scans were signal-averaged to reduce the noise.

Magnetic susceptibility measurements. According to Evans' NMR method, 1 mL of a mixture of 95/5 v/v $C_6D_6$ and cyclohexane was prepared and a portion (0.5 mL) of this solution was transferred to an NMR tube. The other portion (0.5 mL) of this solution was used to dissolve a small amount of iron complex (0.5 mg) and this was transferred in a capillary inserted into the tube. The difference in chemical shift of the cyclohexane protons between the insert and the NMR tube solution at room temperature was used to calculate the molar susceptibility. The data were corrected for the diamagnetism of all atoms.[65]

Dalton Trans., 2018, 47, 13229–13238 - DOI: 10.1039/c8dt03169j



**Synthetic procedures**

The ligands were prepared according to published procedures.[66-68] The identity of the compounds was determined by $^1$H NMR. Complexes **1**, **2** and **4** were synthesized by slightly modified literature procedures.[47,54,56] Synthetic details and full characterization is reported in the ESI.

**Synthesis of SalalenFeCl complex 3**. To a methanol solution (10 mL) of anhydrous iron chloride $FeCl_3$ (63.8 mg, 3.93 x $10^{-4}$ mol) was added a methanol solution (10 mL) of salalen ligand (200 mg, 3.93 x $10^{-4}$ mol)). Triethylamine (0.109 mL, 7.86 x $10^{-4}$) was added to give a dark violet solution. The resulting mixture was stirred for 2 h. Next, the solvent was removed under vacuum. The solid product was dissolved in acetone and filtered through Celite three times. Removal of solvent under vacuum yielded a violet powder, 88%. Characterization of salalenFeCl was done by means of IR- and UV-vis-spectroscopy, MALDI-ToF mass spectrometry and Evans NMR technique. IR (KBr, $cm^{-1}$)): 2952 (C-H Aromatic), 1614 (C=N), 1539, 1461, 1438, 1387, 1378, 1358, 1304, 1256, 1202, 1173, 1076, 1035, 963, 878, 838, 811, 784, 747, 609, 560, 537 (Fe-N), 479 (Fe-O). UV–vis ($CH_3CN$, 0.08 mM, 25 °C, ε = L $mol^{-1}$ $cm^{-1}$): 240 nm (ε = 20575), 270 nm (ε = 14300), 329 nm (ε = 7769), 524 nm (ε = 3853). MS (MALDI-ToF) m/z (ion): 597,289 (FeCl[salalen]$^{\cdot+}$), 562,321 (Fe[salalen]$^{\cdot+}$). Magnetic moment (298 K) $\mu_{eff}$ = 5.31 $\mu_B$.

**General procedure for $CO_2$/ epoxide reaction**

Crystals of complex **3** were obtained by slow evaporation of acetone. A single crystal suitable for X-ray analysis was glued on a glass fiber and mounted on a goniometer head. Diffraction data for **3** were collected at room temperature with a Bruker D8 Quest diffractometer equipped with an PHOTON detector using Cu Kα radiation.

Data reduction was performed with the crystallographic package APEX3.[69] Data were corrected for Lorentz, polarization and absorption.

The structure was solved by direct methods using the program SIR2014[70] and refined by means of full matrix least-squares based on $F^2$ using the program SHELXL.[71]

All non-hydrogen atoms were refined anisotropically, hydrogen atoms were positioned geometrically and included in structure factors calculations but not refined. A total of 366 refinable parameters were finally considered, final disagreement indices: $R1$ = 0.0305 for 5874 reflections with $I > 2\sigma_I$, $_wR2$ = 0.0866 for all 6369 reflections, GooF=1.031. Maximum and minimum residual density were respectively 0.25 and -0.37 e Å$^{-3}$. OLEX2 was used as GUI and also to draw ORTEP figures.[72]

Crystal data: Formula $FeC_{33}H_{50}ClN_2O_2$, FW=598.05, monoclinic, $P2_1/n$, $a$ =17.283(6)Å, $b$ = 9.770(9) Å, $c$ = 19.505(7) Å, $\beta$ = 93.56(3)°, $V$ = 3287(3) Å$^3$, $Z$ = 4, $D_x$ = 1.208 g $cm^{-3}$, μ= 4.648 $mm^{-1}$, $F$(000)=1284.

**General procedure for $CO_2$/ epoxide reaction**

A representative procedure for the $CO_2$/epoxide reaction is described as follows. The reaction was carried out using a ratio epoxide/complexes of 4000 and TBAB/complex = 1 ÷ 4. In a glove-box, catalyst (0.0175 mmol) and co-catalyst (TBAB) were dissolved in the epoxide (4000 equiv, 70 mmol) and then transferred into a autoclave. The autoclave was pressurized to the appropriate pressure of $CO_2$, and the mixture was allowed to stir at the desired temperature for the necessary reaction time. After the prescribed time, the reaction mixture was quenched by immersing the autoclave in an ice bath, opened at air and a small sample of the crude reaction mixture was used to calculate the conversion of epoxide into cyclic carbonate by $^1$H NMR spectroscopy.

**General procedure for L-lactide polymerization**

In a typical experiment, in a glove-box, L-lactide (1.7 mmol, 0.248 g), the catalyst (0.017 mmol) and, when used, co-catalyst (PPNCl, 0.017 mmol, 9.88 x $10^{-3}$ g) were dissolved in toluene or propylene oxide (2 mL) and then transferred into a tube. The tube was heated at 60°C and stirred for the necessary reaction time. After the prescribed time the tube was cooled to room temperature and a $^1$H NMR spectrum of the crude reaction mixture was used to calculate the conversion. The polymer was isolated by precipitation in methanol. NMR spectroscopy ($CDCl_3$) was used to determine molecular weights ($M_n$) of the polymers.

**General procedure for ε-caprolactone polymerization**

In a typical experiment, in a glove-box, the monomer (1.7 mmol, 0.196 g) the catalyst (0.017 mmol) and the cocatalyst (PPNCl, 0.017 mmol, 9.88 x $10^{-3}$ g) were dissolved in PO (1 mL) and then transferred into a vial. The resulting mixture was stirred at room temperature for the necessary reaction time. After the prescribed time, the crude reaction mixture was used to calculate the conversion by $^1$H NMR spectroscopy. The polymer was isolated by precipitation in hexane. NMR spectroscopy ($CDCl_3$) and GPC (THF) were used to determine molecular weights of the obtained polymers.

## Conclusions

Salan, salen and salalen iron(III) complexes have been synthesized and fully characterized. Their behaviour has been compared in the $CO_2$/epoxide reactions and in the ring opening polymerization of L-LA and ε-CL. The reaction of $CO_2$ with three different epoxides (propylene oxide, cyclohexene oxide and styrene oxide) gave the corresponding cyclic carbonate products selectively. The order of reactivity was the following: salanFeCl complex **1** > salenFeCl complex **2**> salalenFeCl complex **3**. This order was explained taking into account the differences in the geometries of the three complexes. In particular, the highest activity of the salanFeCl complex was related to its distorted square planar geometry which leaves enough room in the *trans* position to the chloride, to easily allocate the reacting epoxide. On the other hand, for the salalanFeCl, the chloride occupies an equatorial position of a distorted trigonal bipyramidal geometry thus leaving a reduced coordinative space for the incoming epoxide. The ROP of the ε-CL was carried out by using PO as initiator, to form, *in situ*, an active alkoxide species. As a

consequence, the initiation step of the polymerization reaction is the same reaction occurring in the $CO_2$/epoxide coupling. However, for the ROP, this reaction is not the rate limiting step, thus it determines the rate of the initiation reactions but not the activities of the complexes. The order of activity observed in the ROP of ε-CL was salanFeCl **1** > salalenFeCl **3** > salenFeCl **2** coinciding with the order of the acidity of the metal centers in the different complexes. Finally, in the ROP of L-LA, only the salenFeCl complex **2** proved to be active. We propose that the more acidic complexes **1** and **3** form stable lactate intermediates which hamper the polymerization events.

## Conflicts of interest

There are no conflicts to declare.

## Acknowledgements

The authors acknowledge the Cariplo Foundation (Apollo project 2016-0643) for financial support, Dr. Patrizia Iannece for MALDI-ToF analysis, Dr. Patrizia Oliva for NMR technical assistance and Dr. Mariagrazia Napoli for GPC measurements.

## Notes and references

‡ Molecular weight of the obtained polylactide determined by $^1$H NMR analysis resulted lower than that expected considering the converted equivalents of monomer. This could be due to transesterification reactions promoted by protic impurities coming from the monomer or by a propensity of the iron complex to give these side reactions.

1 P. T. Anastas and J. C. Warner, Green Chemistry: Theory and Practice, Oxford University Press: New York, 1998, p.30.
2 M. Cokoja, C. Bruckmeier, B. Rieger, W. A. Herrmann and F. E. Kuhn, *Angew. Chem., Int. Ed.*, 2011, **50**, 8510-8537.
3 P. P. Pescarmona and M. Taherimehr, *Catal. Sci. Technol.*, 2012, **2**, 2169-2187.
4 Q. Liu, L, Wu, R. Jackstell and M. Beller, *Nat. Commun.*, 2015, **6**, 5933-5948.
5 C. Martìn, G. Fiorani and A. K. Kleij, *ACS Catal.*, 2015, **5**, 1353-1370.
6 Q.-W. Song, Z.-H. Zhoua and L.-N. He, *Green Chem.*, 2017, **19**, 3707-3728.
7 J. Artz, T. E. Müller, K. Thenert, J. Kleinekorte, R. Meys, A, Sternberg, A. Bardow and W. Leitner, *Chem. Rev.*, 2018, **118**, 434-504.
8 A.-C. Albertsson and I. K. Varma, *Biomacromolecules*, 2003, **4**, 1466-1486.
9 R. H. Platel, L. M. Hodgson and C. K. Williams, *Polym. Rev.*, 2008, **48**, 11-63.
10 A. Arbaoui and C. Redshaw, *Polym. Chem.*, 2010, **1**, 801-826.
11 Raquez, J. M.; Mincheva, R.; Coulembier, O.; Dubois, P. 4.31 - Ring-Opening Polymerization of Cyclic Esters: Industrial Synthesis, Properties, Applications, and Perspectives A2 - Matyjaszewski, Krzysztof. In Polymer Science: A Comprehensive Reference; Möller, M., Ed.; Elsevier: Amsterdam, 2012; pp 761−778.
12 R. P. Brannigan and A. P. Dove, *Biomat. Sci.*, 2017, **5**, 9-21.
13 X. Zhang, M. Fevre, G. O. Jones and R. M. Waymouth, *Chem. Rev.*, 2018, **118**, 839−885.
14 I. Bauer and H.-J. Knçlker, *Chem. Rev.*, 2015, **115**, 3170-3387.
15 A. Buchard, M. R. Kember, K. G. Sandemanb and C. K. Williams, *Chem. Commun.*, 2011, **47**, 212–214.
16 C. J. Whiteoak, E. Martin, M. Martinez Belmonte, J. Benet-Buchholz and A. W. Kleij, *Adv. Synth. Catal.*, 2012, **354**, 469-476.
17 C. J. Whiteoak, B. Gjoka, E. Martin, M. M. Belmonte, E. C. Escudero-Adán, C. Zonta, G. Licini and A. W. Kleij, *Inorg. Chem.*, 2012, **51**, 10639–10649.
18 M. Taherimehr, S. M. Al-Amsyar, C. J. Whiteoak, A. W. Kleij and P. P. Pescarmona, *Green Chem.*, 2013, **15**, 3083–3090.
19 M. Taherimehr, J. P. C. C. Sertã, A. W. Kleij, C. J. Whiteoak and P. P. Pescarmona, *ChemSusChem*, 2015, **8**, 1034–1042.
20 A. Buonerba, A. De Nisi, A. Grassi, S. Milione, C. Capacchione, S. Vagin and B. Rieger, *Catal. Sci. Technol.*, 2015, **5**, 118–123.
21 F. Della Monica, S. V. C. Vummaleti, A. Buonerba, A. De Nisi, M. Monari, S. Milione, A. Grassi, L. Cavallo, C. Capacchione *Adv. Synth. Catal.* 2016, **358**, 3231-3243.
22 F. A. Al-Qaisi, N. Genjang, M. Nieger and T. Repo, *Inorg. Chim. Acta*, 2016, **442**, 81−85.
23 M. Sunjuk, A. S. Abu-Surrah, E. Al-Ramahi, A. K. Qaroush and A. Saleh, *Transition. Met. Chem.*, 2013, **38**, 253-257.
24 C. K. Karan and M. Bhattacharjee, *Inorg. Chem.*, 2018, **57**, 4649−4656.
25 O. Martínez-Ferraté, J. M. López-Valbuena, M. Martínez Belmonte, A. J. P. White, J. Benet-Buchholz, G. J. P. Britovsek, C. Clave and P. W. N. M. van Leeuwen, *Dalton Trans.*, 2016, **45**, 3564–3576.
26 F. Chen, N. Liu and B. Dai, *ACS Sustainable Chem. Eng.*, 2017, **5**, 9065−9075
27 J. E. Dengler, M. W. Lehenmeier, S. Klaus, C. E. Anderson, E. Herdtweck and B. Rieger, *Eur. J. Inorg. Chem.*, 2011, **2011**, 336–343.
28 X. Sheng, L. Qiao, Y. Qin, X. Wang and F. Wang, *Polyhedron*, 2014, **74**, 129–133.
29 M. A. Fuchs, T. A. Zevaco, E. Ember, O. Walter, I. Held, E. Dinjus and M. Doring, *Dalton Trans.*, 2013, **42**, 5322–5329.
30 H. Büttner, C. Grimmer, J. Steinbauer and T. Werner, *ACS Sustainable Chem. Eng.*, 2016, **4**, 4805−4814.
31 A. Södergård and M. Stolt, *Macromol. Symp.*, 1998, 130, 393–402.
32 R. R. Gowda and D. Chakraborty, *J. Mol. Catal. A: Chem.*, 2009, **301**, 84–92.
33 C. S. Hege and S. M. Schiller, *Green Chem.*, 2014, **16**, 1410–1416.
34 M. Stolt and A. Södergård, *Macromolecules*, 1999, **32**, 6412–6417.
35 B. J. O'Keefe, S. M. Monnier, M. A. Hillmyer and W. B. Tolman, *J. Am. Chem. Soc.*, 2001, 123, 339–340.
36 D. S. McGuinness, E. L. Marshall, V. C. Gibson and J. W. Steed, *J. Polym. Sci., Part A: Polym. Chem.*, 2003, 41, 3798–3803.
37 X. Wang, K. Liao, D. Quan and Q. Wu, *Macromolecules*, 2005, 38, 4611–4617.
38 H. R. Kricheldorf and D.-O. Damrau, *Macromol. Chem. Phys.*, 1997, **198**, 1767–1774.
39 B. J. O'Keefe, L. E. Breyfogle, M. A. Hillmyer and W. B. Tolman, *J. Am. Chem. Soc.*, 2002, 124, 4384–4393.
40 A. B. Biernesser, B. Li and J. A. Byers, *J. Am. Chem. Soc.*, 2013, **135**, 16553–16560.
41 C. Geng, Y. Peng, L. Wang, H. W. Roesky and K. Liu, *Dalton Trans.*, 2016, **45**, 15779-16782.
42 Y.-Y. Fang, W.-J. Gong, X.-J. Shang, H.-X. Li, J. Gao and J.-P. Lang, *Dalton Trans.*, 2014, **43**, 8282–8289
43 V. C. Gibson, E. L. Marshall, D. Navarro-Llobet, A. J. P. White and D. J. Williams, *J. Chem. Soc., Dalton Trans.*, 2002, 4321–4322.

44 A. Arbaoui, C. Redshaw, M. R. J. Elsegood, V. E. Wright, A. Yoshizawa and T. Yamato, *Chem. – Asian J.*, 2010, **5**, 621–633.
45 M. Z. Chen, H. M. Sun, W. F. Li, Z. G. Wang, Q. Shen and Y. Zhang, *J. Organomet. Chem.*, 2006, **691**, 2489–2494.
46 A. S. Abu-Surrah, H. M. Abdel-Halim, H. A. N. Abu-Shehab and E. Al-Ramahi, *Transit Met Chem*, 2017, **42**, 117-122.
47 R. Duan, C. Hu, X. Li, X. Pang, Z. Sun, X. Chen and X. Wang, *Macromolecules*, 2017, **50**, 9188-9195.
48 D. Alhashmialameer, J. Collins, K. Hattenhauera and F. M. Kerton, *Catal. Sci. Technol.*, 2016, **6**, 5364-5373.
49 A. Pilone, K. Press, I. Goldberg, M. Kol, M. Mazzeo, M. Lamberti, *J. Am. Chem. Soc.*, 2014, **136**, 2940-2943.
50 A. Pilone, N. De Maio, K. Press, V. Venditto, D. Pappalardo, M. Mazzeo, C. Pellecchia, M. Kol, M. Lamberti, *Dalton Trans.*, 2015, **44**, 2157-2165.
51 F. Isnard, M. Lamberti, L. Lettieri, I. D'Auria, K. Press, R. Troiano, M. Mazzeo, *Dalton Trans.*, 2016, **45**, 16001–16010.
52 M. Cozzolino, K. Press, M. Mazzeo, M. Lamberti, *ChemCatChem*, 2016, **8**, 455–460.
53 M. Cozzolino, T. Rosen, I. Goldberg, M. Mazzeo, M. Lamberti, *ChemSusChem*, 2017, **10**, 1217-1223.
54 K. Hasan, C. Fowler, P. Kwong, A. K. Crane, J. L. Collins and C. M. Kozak, *Dalton Trans.*, 2008, 2991–2998.
55 J. B. H. Strautmann, S. DeBeer George, E. Bothe, E. Bill, T. Weyhermuller, A. Stammler, H. Bogge and T. Glaser, *Inorg. Chem.*, 2008, **47**, 6804-6824.
56 S. Liao and B. Lista, *Adv. Synth. Catal.* 2012, **354**, 2363-2367.
57 A. M. Aslam, S. Rajagopal, M. Vairamani, M. Ravikumar, *Transition Met Chem*, 2011, **36**, 751-759.
58 M. H. Chisholm, D. Navarro-Llobet and W. J. Simonsick, *Macromolecules*, 2001, **34**, 8851-8857.
59 S. Doherty, R. J. Errington, N. Housley and W. Clegg, *Organometallics*, 2004, **23**, 2382-2388.
60 M. Anker, C. Balasanthiran, V. Balasanthiran, M. H. Chisholm, S. Jayaraj, K. Mathieu, P. Piromjitpong, S. Praban, B. Raya and W. J. Simonsick, Jr, *Dalton Trans.*, 2017, **46**, 5938-5945.
61 D. D. Darensbourg, *Chem. Rev.*, 2007, **107**, 2388-2410.
62 S. Klaus, M. W. Lehenmeier, C. E. Anderson and B. Rieger, *Coord. Chem. Rev*., 2011, **255**, 1460-1479.
63 A. Decortes, A. M. Castilla and A. W. Kleij, *Angew. Chem. Int. Ed.*, 2010, **49**, 9822-9837.
64 K. R. Delle Chiaie, A. B. Biernesser, M. A. Ortuño, B. Dereli, D. A. Iovan, M. J. T. Wilding, B. Li, C. J. Cramer and J. A. Byers, *Dalton Trans.*, 2017, **46**, 12971-12980.
65 G. A. Bain and J. F. Berry, *J. Chem. Educ.*, 2008, **85**, 532-536.
66 E. Y. Tshuva, N. Gendeziuk and M. Kol, *Tetrahedron Letters*, 2001, **42**, 6405-6407.
67 P. Hormnirun, E. L. Marshall, V. C. Gibson, R. I. Pugh and A. J. P. White, *PNAS*, 2006, **103**, 15343-15348.
68 A. Yeori, S. Gendler, S. Groysman, I. Goldberg, M. Kol, *Inorg. Chem. Commun.*, 2004, **7**, 280-282.
69 *APEX3*, *SAINT* and *SADABS*, Bruker 2015. Bruker AXS Inc, Madison , Wisconsin, USA.
70 M. C. Burla, R. Caliandro, B. Carrozzini, G. L. Cascarano, C. Cuocci, C. Giacovazzo, M. Mallamo, A. Mazzone and G. Polidori, *J. Appl. Cryst.*, 2015, **48**, 306–309.
71 G. M. Sheldrick, *Acta Cryst.*, 2015, **C71**, 3–8.
72 O. V. Dolomanov, L. J. Bourhis, R. J. Gildea, J. A. K. Howard and H. Puschmann, *J. Appl. Cryst.*, 2009, **42**, 339–341.